

“© 2020 IEEE. Personal use of this material is permitted. Permission from IEEE must be obtained for all other uses, in any current or future media, including reprinting/republishing this material for advertising or promotional purposes, creating new collective works, for resale or redistribution to servers or lists, or reuse of any copyrighted component of this work in other works.”

# Wireless Powered Intelligent Reflecting Surfaces for Enhancing Wireless Communications

Yuze Zou, Shimin Gong, Jing Xu, Wenqing Cheng, Dinh Thai Hoang and Dusit Niyato

**Abstract**—Recently, the intelligent reflecting surface (IRS) has become a promising technology for energy- and spectrum-efficient communications by reconfiguring the radio environment. In this paper, we consider multiple-input single-output (MISO) transmissions from a multi-antenna access point (AP) to a receiver, assisted by a practical IRS with a power budget constraint. The IRS can work in energy harvesting and signal reflecting phases. It firstly harvests RF energy from the AP’s signal beamforming and then uses it to sustain its operations in the signal reflecting phase. We aim to characterize the maximum capacity by optimizing the AP’s transmit beamforming, the IRS’s time allocation in two operational phases, and the IRS’s passive beamforming to enhance the information rate. To solve the non-convex maximization problem, we exploit its structural properties and decompose it into two sub-problems in two phases. The IRS’s phase shift optimization in the reflecting phase follows a conventional passive beamforming problem to maximize the received signal power. In the energy harvesting phase, the IRS’s time allocation and the AP’s transmit beamforming are jointly optimized using monotonic optimization. Simulation results verify the effectiveness of the proposed algorithm.

**Index Terms**—Energy harvesting, wireless powered transfer, time switching protocol, intelligent reflecting surface.

## I. INTRODUCTION

Recently, Intelligent reflecting surface (IRS) has become one of the most promising solutions to improve energy- and spectrum-efficiency (EE/SE) of wireless communications, by

Copyright (c) 2020 IEEE. Personal use of this material is permitted. However, permission to use this material for any other purposes must be obtained from the IEEE by sending a request to pubs-permissions@ieee.org.

Yuze Zou, Jing Xu, and Wenqing Cheng are with School of Electronic Information and Communications, Huazhong University of Science and Technology, China. Shimin Gong is with School of Intelligent Systems Engineering, Sun Yat-sen University, China, and also with Pengcheng Laboratory, Shenzhen, China. Dinh Thai Hoang is with School of Electrical and Data Engineering, University of Technology Sydney, Australia. Dusit Niyato is with School of Computer Science and Engineering, Nanyang Technological University, Singapore. (Corresponding author: Shimin Gong, e-mail: gongshm5@mail.sysu.edu.cn)

The work of Yuze Zou was supported in part by National Natural Science Foundation of China under Grant 61977064. The work of Shimin Gong was supported in part by the National Natural Science Foundation of China under Grant 61972434, in part by the Shenzhen Basic Research Program under Grant JCYJ20190807154009444, in part by the Shenzhen Talent Peacock Plan Program under Grant KQTD2015071715073798, and in part by the PCL Future Greater-Bay Area Network Facilities for Largescale Experiments and Applications (LZC0019). The work of Dusit Niyato was supported by the National Research Foundation (NRF), Singapore, under Singapore Energy Market Authority (EMA), Energy Resilience, NRF2017EWT-EP003-041, Singapore NRF2015-NRF-ISF001-2277, Singapore NRF National Satellite of Excellence, Design Science and Technology for Secure Critical Infrastructure NSoE DeST-SCI2019-0007, A\*STAR-NTU-SUTD Joint Research Grant on Artificial Intelligence for the Future of Manufacturing RGANS1906, Wallenberg AI, Autonomous Systems and Software Program and Nanyang Technological University (WASP/NTU) under grant M4082187 (4080), and NTU-WeBank JRI (NWJ-2020-004).

providing the capability of reconfiguring the radio environment in favor of information transmission, e.g., [1] and [2]. The IRS is a planar array consisting of numerous passive scattering elements. Each scattering element is able to induce an electronically-controlled phase shift independently on the incident electromagnetic wave. The joint control of all scattering elements’ phase shifts, namely, passive beamforming, can reshape the physical channel on demand, e.g., focusing the signal beams at designated receiver and suppressing interference to undesirable directions. The main advantage of IRS-enhanced wireless communications lies in that it can greatly increase the channel capacity, with extremely low power consumption and flexibility for large-scale deployment in the radio environment.

The IRS’s passive beamforming along with the transmission control of the legacy transceivers is envisioned to revolutionize the network optimization paradigm. The existing research works on IRS-assisted wireless networks mainly focus on maximization of the channel capacity [3], [4], energy efficiency [5], or minimization of the AP’s transmit power [6]. The physical layer security can also be enhanced by leveraging the IRS’s passive beamforming [7], [8]. However, the IRS’s energy consumption is usually ignored due to the extremely low power consumption of the passive scattering elements. In fact, the IRS’s energy consumption depends on the size and implementation of its scattering elements [5]. For a self-sustainable IRS, it has to harvest energy from the RF signals, which is also featured with extremely low energy-conversion efficiency. As such, the IRS’s energy consumption becomes a critical design aspect for overall performance improvement.

In this paper, we envision a wireless network assisted by a self-sustainable IRS capable of harvesting energy from RF signals, similar to the RF-powered backscatter-aided relay communications [9]. To sustain the IRS’s operations, the IRS controller can schedule its switching between the energy harvesting and signal reflecting phases, similar to the conventional time-switching (TS) protocol for energy harvesting IoT devices [10]. As depicted in Figure 1, the signal transmission from the multi-antenna AP to the single-antenna receiver is assisted by the energy harvesting IRS. The IRS firstly operates in the energy harvesting phase to charge its capacitors for a portion of the time slot, and then works in the reflecting phase by tuning its phase shifts to assist signal transmissions from the AP to the receiver. We aim to optimize the AP’s transmit beamforming in two phases, the IRS’s phase shifts and time allocation to maximize the transmission rate. The AP’s transmit beamforming in the first phase not only determines the data rate to the receiver, but also affects the energy flow to the IRS. This implies a close

coupling between the AP's transmit beamforming and the IRS's time allocation in two phases. The solution to the non-convex maximization problem is decomposed into two sub-problems. The sub-problem in the second phase follows a conventional passive beamforming optimization [6]. As for the first phase, by exploiting the problem structure, we devise the monotonic optimization algorithm to find the optimal time allocation and transmit beamforming strategies. To the best of our knowledge, we are the first to characterize the maximum rate in an IRS-assisted MISO system, where the IRS works in a self-sustainable manner under TS protocol. Simulation results verify the potential performance gain of the proposed system and reveal that the performance gain becomes more significant with higher transmit power.

## II. SYSTEM MODEL AND FORMULATION

We consider the IRS-assisted MISO downlink system, as shown in Fig. 1, where the AP with  $M$  antennas transmits information to the single-antenna receiver device. The IRS with  $N$  passive scattering elements is capable of adjusting phase shifts dynamically according to the channel state information (CSI). The IRS controller is also equipped with an energy harvester circuit that is able to harvest RF energy from the AP's beamforming signals. We assume that the IRS controller can switch the IRS's operations in two phases, i.e., the energy harvesting phase and the signal reflecting phase. The complex channels of the AP-receiver, AP-IRS, and IRS-receiver links are denoted by  $\mathbf{h}_d \in \mathbb{C}^{M \times 1}$ ,  $\mathbf{G} \in \mathbb{C}^{N \times M}$  and  $\mathbf{h}_r \in \mathbb{C}^{N \times 1}$ , respectively. Let  $\Theta = \text{diag}(e^{j\theta_1}, \dots, e^{j\theta_N})$  denote phase shift matrix for the IRS, where  $\theta_n \in [0, 2\pi)$ ,  $n \in \{1, \dots, N\}$  denotes the phase of the reflection coefficient of the  $n$ -th scattering element. Vectors are denoted by bold lowercase letters while matrices are denoted by bold uppercase letters.  $\|\cdot\|$  denotes the Euclidean norm of a complex vector.  $\text{Tr}(\mathbf{X})$  denotes the trace of matrix  $\mathbf{X}$  and  $\text{diag}(\mathbf{a})$  denotes the diagonal matrix with the diagonal vector  $\mathbf{a}$ .

### A. IRS-assisted and Unassisted Transmission Rates

Without loss of generality, we focus on the AP's signal transmission in a unit time slot. Considering the TS protocol similar to [10], the IRS is individually scheduled by the IRS controller to operate in two phases. The AP's information transmission is similarly divided into two phases, i.e., unassisted and IRS-assisted transmissions, as illustrated in Fig. 1. In the first phase with duration  $1 - t$ , the IRS harvests RF energy from the AP's signal beamforming to the receiver. In the second phase  $t$ , the IRS adapts its passive beamforming and thus reflects the incident signal to enhance information transmission from the AP to the receiver. The AP can also adjust its transmit beamforming vectors in two phases, denoted as  $\mathbf{w}_1$  and  $\mathbf{w}_2 \in \mathbb{C}^{M \times 1}$  respectively, to balance the energy transfer to the IRS and the information transfer to the receiver. Let  $s$  denote the complex symbol transmitted by the AP with unit power. In the first phase, the received signal is given by  $y = \mathbf{h}_d^H \mathbf{w}_1 s + \nu_d$  (the superscript  $H$  denotes the conjugate transpose operation), where  $\nu_d \sim \mathcal{CN}(0, \sigma^2)$  denotes the noise

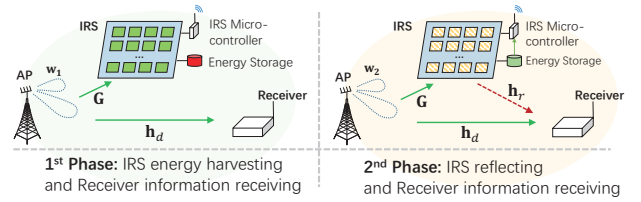


Figure 1: An MISO system assisted by a self-sustainable IRS.

signal with zero mean and variance  $\sigma^2$ . Hence, the data rate in the first phase is given by

$$r_1(\mathbf{w}_1) = \log_2(1 + |\mathbf{h}_d^H \mathbf{w}_1|^2 / \sigma^2). \quad (1)$$

Similarly, the data rate in the second phase is given by

$$r_2(\mathbf{w}_2, \Theta) = \log_2(1 + |(\mathbf{h}_d + \mathbf{G}^H \Theta \mathbf{h}_r)^H \mathbf{w}_2|^2 / \sigma^2), \quad (2)$$

where  $\mathbf{h}_d + \mathbf{G}^H \Theta \mathbf{h}_r$  represents the enhanced channel from the AP to the receiver by the IRS's passive beamforming  $\Theta$ .

### B. Wireless Powered Self-sustainable IRS

The harvested energy by the IRS in the first phase can be stored in capacitors and shared among all elements to ensure their operations during the second phase. In the first phase, the incident signal at the IRS is given by  $\mathbf{x} = \mathbf{G} \mathbf{w}_1 s$ , which is fed into the IRS's energy harvester. Hence, the harvested energy by the IRS is given by  $\eta(1 - t) \|\mathbf{G} \mathbf{w}_1\|^2$ , where  $\eta$  denotes the energy harvesting efficiency. In the second phase, the IRS fully reflects the incident signals from the AP to the receiver by adjusting its passive beamforming  $\Theta$ . The IRS's power consumption in the second phase relates to  $N$ , the number of scattering elements, and the phase resolution of each scattering element. Typically, the IRS power consumption increases linearly with the IRS's size and also depends on the phase resolution of individual reflecting element, e.g., [11], [12]. As such, the IRS's energy budget constraint is given by  $\eta(1 - t) \|\mathbf{G} \mathbf{w}_1\|^2 \geq tN\mu$ , where  $\mu$  denotes the power consumption of a single scattering element and it relates to the phase resolution. Note that we can install multiple energy harvesters in the physical structure of a large-scale IRS to improve the energy harvesting efficiency. In the special case, each scattering element can have sensing capability and harvest energy individually. Then, the power budget can be simplified as  $\eta(1 - t) \|\mathbf{G} \mathbf{w}_1\|^2 \geq t\mu$ .

## III. THROUGHPUT MAXIMIZATION IN TWO PHASES

We assume that the AP can communicate with the IRS and thus jointly adapt their operating parameters in two phases to maximize the throughput from the AP to the receiver. Note that the AP's transmit beamforming also transfers energy to the IRS in the first phase. Hence, it is necessary to optimize different beamforming strategies  $\mathbf{w}_1$  and  $\mathbf{w}_2$  in two phases. The time division  $t$  between two phases is also a critical parameter that balances the IRS's power demand and supply. The throughput maximization problem is formulated as:

$$(\mathbf{P1}) \quad \max_{t \geq 0, \mathbf{w}_1, \mathbf{w}_2, \Theta} (1 - t)r_1(\mathbf{w}_1) + t \cdot r_2(\mathbf{w}_2, \Theta) \quad (3a)$$

$$\text{s.t.} \quad (1 - t)\eta \|\mathbf{G} \mathbf{w}_1\|^2 \geq tN\mu, \quad (3b)$$

$$\|\mathbf{w}_1\|^2 \leq p_{\max}, \|\mathbf{w}_2\|^2 \leq p_{\max}, \quad (3c)$$

where  $r_1(\mathbf{w}_1)$ ,  $r_2(\mathbf{w}_2, \Theta)$ , defined in (1) and (2), represent the data rates in the first and the second phases, respectively.  $p_{\max}$  denotes the AP's maximum transmit power. Constraint (3b) denotes the IRS's power budget, which depends on the AP's transmit beamforming  $\mathbf{w}_1$  in the first phase and the IRS's time switching strategy.

#### A. Decomposed Solution Method

Problem (P1) is generally non-convex due to couplings among decision variables in both the objective and constraints. To tackle this difficulty, we decompose the problem into two sub-problems by exploiting its structural properties. Firstly, we note that  $\mathbf{w}_2$  and  $\Theta$  only appear in the objective (3a) and  $\mathbf{w}_2$  is individually constrained by the AP's power limit. Hence, the maximization of  $r_2(\mathbf{w}_2, \Theta)$  can be decomposed from problem (P1) and formulated as the following sub-problem:

$$\text{(P1.1)} \quad \bar{\gamma}_2 \triangleq \max_{\Theta, \mathbf{w}_2} |(\mathbf{h}_d + \mathbf{G}^H \Theta \mathbf{h}_r)^H \mathbf{w}_2|^2 / \sigma^2 \quad (4a)$$

$$\text{s.t.} \quad \|\mathbf{w}_2\|^2 \leq p_{\max}, \quad (4b)$$

$$0 \leq \theta_n < 2\pi, \forall n \in \{1, \dots, N\}, \quad (4c)$$

where  $\bar{\gamma}_2$  denotes the maximum SNR in the second phase by jointly optimizing the AP's transmit beamforming and the IRS's passive beamforming. Hence, the maximum data rate in the second phase is given by  $\bar{r}_2 = \log_2(1 + \bar{\gamma}_2)$ . Given the solution to (P1.1), problem (P1) can be simplified as

$$\max_{t, \mathbf{w}_1} (1-t)r_1(\mathbf{w}_1) + t \cdot \bar{r}_2 \quad (5a)$$

$$\text{s.t.} \quad (3b) \text{ and } \|\mathbf{w}_1\|^2 \leq p_{\max}. \quad (5b)$$

Note that we have  $\bar{r}_2 > r_1$  due to the channel enhancement by the IRS in the second phase. As such, we can easily verify that the power budget constraint (3b) will hold with equality at optimum of problem (5). Otherwise, we can properly increase  $t$  in (3b) to further increase the objective in (5a). Therefore, the optimal time division  $t^*$  is given as follows:

$$t^*(\mathbf{w}_1) = \frac{\eta \|\mathbf{G}\mathbf{w}_1\|^2}{N\mu + \eta \|\mathbf{G}\mathbf{w}_1\|^2}. \quad (6)$$

By substituting (6) into the objective (5a), we are expected to solve the second sub-problem (P1.2):

$$\text{(P1.2)} \quad \max_{\mathbf{w}_1} (1-t^*(\mathbf{w}_1))r_1(\mathbf{w}_1) + t^*(\mathbf{w}_1)\bar{r}_2 \quad (7a)$$

$$\text{s.t.} \quad \|\mathbf{w}_1\|^2 \leq p_{\max}. \quad (7b)$$

Problem (P1.1) is similar to the joint active and passive beamforming optimization problem studied in the literature, e.g., [6], which can follow the conventional semidefinite relaxation (SDR) method. The second problem (P1.2) introduces the couplings between the AP's transmit beamforming and the IRS's time allocation strategies. In the sequel, we present detailed solutions to these two sub-problems, respectively.

#### B. Rate Maximization for IRS-assisted Transmission

Given a fixed  $\Theta$ , the AP's optimal beamforming vector  $\mathbf{w}_2$  can be simply aligned with the enhanced channel  $\mathbf{h}_d + \mathbf{G}^H \Theta \mathbf{h}_r$  via maximum-ratio transmission (MRT), i.e.,

$$\mathbf{w}_2^* = \sqrt{p_{\max}} (\mathbf{h}_d + \mathbf{G}^H \Theta \mathbf{h}_r) / \|\mathbf{h}_d + \mathbf{G}^H \Theta \mathbf{h}_r\|. \quad (8)$$

As such, problem (P1.1) is reduced to

$$\max_{\Theta} \|\mathbf{h}_d + \mathbf{G}^H \Theta \mathbf{h}_r\|^2 \quad \text{s.t.} \quad (4c),$$

by changing variables, let  $\Phi = \text{diag}(\mathbf{h}_r^H) \mathbf{G}$  and  $\nu = [e^{j\theta_1}, \dots, e^{j\theta_N}]^H$ , this problem is equivalent to the following quadratically constrained quadratic program (QCQP).

$$\text{(P2)} \quad \max_{\nu} \quad \nu^H \Phi \Phi^H \nu + \nu^H \Phi \mathbf{h}_d + \mathbf{h}_d^H \Phi \nu + \mathbf{h}_d^H \mathbf{h}_d$$

$$\text{s.t.} \quad |\nu_n| = 1, \forall n = 1, \dots, N.$$

Though problem (P2) is still non-convex, it can be further converted into a semidefinite program (SDP) by semidefinite relaxation (SDR) technique, similar to that in [6]. We omit details here for conciseness. As such, the converted SDP can be solved efficiently by the interior-point algorithms using an off-the-shelf solver, such as CVX [13].

#### C. Optimizing Energy Transfer to the IRS

Problem (P1.2) is still hard to solve in its current form as  $\mathbf{w}_1$  appears in both numerator and denominator in (6). Define  $\gamma_0 = \|\mathbf{G}\mathbf{w}_1\|^2$  for notational convenience, we can rewrite (P1.2) as follows:

$$\max_{\mathbf{w}_1} r(\gamma_0, r_1) \triangleq \bar{r}_2 - \frac{\bar{r}_2 - r_1}{1 + \frac{\eta}{N\mu} \gamma_0} \quad \text{s.t.} \quad \|\mathbf{w}_1\|^2 \leq p_{\max}. \quad (9)$$

Though problem (9) is non-convex, it is easy to verify that the objective  $r(\gamma_0, r_1)$  in (9) is increasing in both  $r_1$  and  $\gamma_0$ , which makes it possible to solve the problem optimally by using the monotonic optimization (MO) algorithm [14]. Specifically, we can further rewrite problem (9) in the following form:

$$\text{(P3)} \quad \max_{(\gamma_0, r_1) \in \Omega} r(\gamma_0, r_1) \quad (10a)$$

$$\text{s.t.} \quad \Omega \triangleq \left\{ (\gamma_0, r_1) \left| \begin{array}{l} \|\mathbf{h}_d^H \mathbf{w}_1\|^2 \geq r_1 \\ \|\mathbf{G}\mathbf{w}_1\|^2 \geq \gamma_0 \\ \|\mathbf{w}_1\|^2 \leq p_{\max} \end{array} \right. \right\}, \quad (10b)$$

where  $\Omega$  is defined as the feasible set of  $(\gamma_0, r_1)$ . Besides monotonicity in the objective  $r(\gamma_0, r_1)$ , we also find that  $\Omega$  bears a special structural property, stated as follows:

**Proposition 1.** *Given any feasible point  $(\gamma_0, r_1) \in \Omega$ , we always have  $(\gamma'_0, r'_1) \in \Omega$  for any  $(\gamma'_0, r'_1) \preceq (\gamma_0, r_1)$ .*<sup>1</sup>

The proof of Proposition 1 is straightforward by showing that there always exists a solution  $\mathbf{w}'_1$  that satisfies the inequalities in (10b). Let  $\mathbf{w}_1$  denote the solution corresponding to  $(\gamma_0, r_1) \in \Omega$ . We can simply construct  $\mathbf{w}'_1$  as  $\mathbf{w}'_1 = \mathbf{w}_1$ . Hence, we have  $r'_1 \leq r_1 \leq \|\mathbf{h}_d^H \mathbf{w}'_1\|^2$  and  $\gamma'_0 \leq \gamma_0 \leq \|\mathbf{G}\mathbf{w}'_1\|^2$ , which implies that  $(\gamma'_0, r'_1) \in \Omega$ . We usually call  $\Omega$  as a normal set if it has the above structural property.

**Proposition 2.** *The optimum of problem (P3) is attained on the boundary of the feasible set  $\Omega$ , denote by  $\partial^+ \Omega$ .*

The proof of Proposition 2 can be easily obtained from the results in [14]. This proposition allows us to apply the MO algorithm to solve problem (P3) optimally in an iterative

<sup>1</sup>  $\mathbf{a} \preceq \mathbf{b}$  means each component of vector  $\mathbf{a}$  is no larger than the corresponding one of vector  $\mathbf{b}$ .

procedure. As the objective  $r(\gamma_0, r_1)$  is monotonic, the maximum is always on the boundary point of the feasible set  $\Omega$ . The appealing structural property of a normal set allows us to find the optimal boundary point efficiently by successive polyblock approximation (SPA). In each iteration, the SPA algorithm uses box sets<sup>2</sup>, namely, polyblock, to approximate the feasible region  $\Omega$ . The algorithm starts from an initial polyblock  $P_0$  that is large enough to cover the feasible set, i.e.,  $P_0 \supset \Omega$ . At  $k$ -th iteration, a smaller polyblock can be created such that  $P_{k-1} \supset P_k \supset \Omega$ .

Let  $V_k$  denote the set of vertices of the polyblock  $P_k$ . Hence, we can update the upper bound on (10) as follows:

$$\max_{(\gamma_0, r_1) \in \Omega} r(\gamma_0, r_1) \leq \max_{(\gamma_0, r_1) \in P_k} r(\gamma_0, r_1) = \max_{(\gamma_0, r_1) \in V_k} r(\gamma_0, r_1).$$

The first inequality holds due to the fact that  $\Omega \subset P_k$  while the equality holds due to the monotonicity of the objective function  $r(\gamma_0, r_1)$ , which always achieves its maximum on one of the vertices points of the polyblock  $P_k$ . Here, we assume that  $\mathbf{v}_k = (\gamma_0^{(k)}, r_1^{(k)}) \in V_k$  achieves the upper bound, given by  $r_U^{(k)} = r(\mathbf{v}_k)$ , in the  $k$ -th iteration. If  $\mathbf{v}_k \in \Omega$ , it is the optimal feasible solution. Otherwise, we can update a lower bound on (10) by projecting the infeasible vertex point  $\mathbf{v}_k$  onto the boundary of  $\Omega$ . In particular, we can find the maximum scaling factor  $\lambda$  such that  $\lambda \mathbf{v}_k \in \Omega$ . Let  $\mathbf{o}_k = \lambda \mathbf{v}_k$  denote the projection point. Thus, we can use  $r_L^{(k)} = r(\mathbf{o}_k)$  as a lower bound on (10) in the  $k$ -th iteration. After that, infeasible polyblock spanned by  $(\mathbf{o}_k, \mathbf{v}_k)$  can be trimmed from  $P_k$  to get a smaller polyblock  $P_{k+1} \supset \Omega$ . This procedure continues until the gap between the lower and upper bounds falls below an error tolerance  $\epsilon$ . The solution procedures are depicted as SPA in Algorithm 1. A similar approach has been applied in conventional wireless powered communications [15].

The computational complexity of the SPA algorithm mainly lies in two parts. One part relates to the outer-loop iterations of the MO algorithm and the other part lies in the solution to SDP problems. The complexity of the MO algorithm is generally increasing exponentially in the dimension of decision variables [14]. However in our formulation, the dimension is limited to 2, which are  $\gamma_0$  and  $\gamma_1$ . This guarantees a fast convergence for the outer-loop iterations. On the other hand, within each loop, the main computational task lies in the projection of an infeasible vertex  $\mathbf{v}_k$  onto the boundary  $\partial^+ \Omega$ , which can be performed in an efficient bisection method. Specifically, given a fixed  $\lambda \in (0, 1]$ , the following feasibility check determines whether to scale down or up  $\lambda$  in the next iteration.

$$\min \quad \|\mathbf{w}_1\|^2 \quad (11a)$$

$$\text{s.t.} \quad |\mathbf{h}_d^H \mathbf{w}_1|^2 \geq r_1 \lambda \text{ and } \|\mathbf{G} \mathbf{w}_1\|^2 \geq \gamma_0 \lambda. \quad (11b)$$

Let  $p(\lambda)$  denote the optimum to problem (11). If  $p(\lambda) \leq p_{\max}$ , this implies that the scaled vertex  $\lambda \mathbf{v}_k = (\lambda \gamma_0, \lambda r_1) \in \Omega$ . Hence, we can increase  $\lambda$  in the next bisection iteration, otherwise we have to decrease it. To solve problem (11) efficiently, we introduce a matrix variable  $\mathbf{W}_1 = \mathbf{w}_1 \mathbf{w}_1^H$  and then transform it into an efficiently tractable SDP via the SDR.

<sup>2</sup>A box set is in the form of  $[\mathbf{0}, \mathbf{v}]$ , where  $\mathbf{v}$  is the end point of the box, and also called a vertex of a polyblock that is the union of finite box sets.

---

### Algorithm 1 Two-stage Algorithm for Problem (P1)

---

#### First Stage: Optimize IRS reflecting phase and AP's $\mathbf{w}_2$

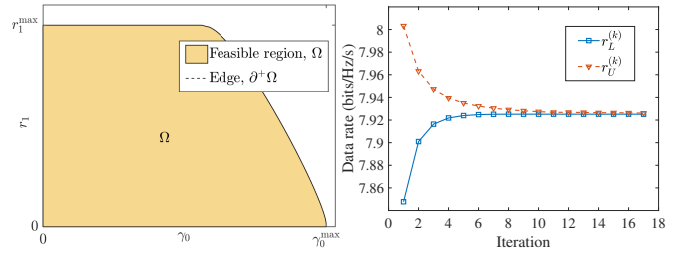
---

- 1: Solve the SDP form of problem (P2)
  - 2: Retrieve  $\mathbf{w}_2^*$  by (8)
- 

#### Second Stage: SPA algorithm for problem (P3)

---

- 3: Initialize  $\gamma_0^{\max}$  and  $r_1^{\max}$ , set  $\mathbf{v}_0 = (\gamma_0^{\max}, r_1^{\max})$
  - 4:  $\epsilon \leftarrow 10^{-5}$ ,  $k \leftarrow 0$ , initialize  $V_0 = \{\mathbf{v}_0\}$  and  $P_0$
  - 5:  $r_L^{(k)} \leftarrow 0$ ,  $r_U^{(k)} \leftarrow r(\mathbf{v}_k)$
  - 6: **while**  $|r_U^{(k)} - r_L^{(k)}| > \epsilon$
  - 7:      $k \leftarrow k + 1$
  - 8:     Find  $\mathbf{v}_k$  that maximizes the objective, i.e.,  
         $\mathbf{v}_k = \arg \max_{\mathbf{v} \in V_k} r(\mathbf{v})$
  - 9:      $r_U^{(k)} \leftarrow r(\mathbf{v}_k)$
  - 10:    Find projection point  $\mathbf{o}_k = \lambda \mathbf{v}_k$  by bisection
  - 11:     $r_L^{(k)} \leftarrow r(\lambda \mathbf{v}_k)$
  - 12:    Update vertex set  $V_{k+1}$  and  $P_{k+1} \leftarrow \cup_{\mathbf{v} \in V_{k+1}} [\mathbf{0}, \mathbf{v}]$
  - 13: **end while**
  - 14: **Output:** AP's beamforming matrix  $\mathbf{W}_1$ .
- 



(a) A normal feasible region of (P3)    (b) Convergence of Algorithm 1

Figure 2: An illustrative example: The feasible region of problem (P3) and the convergence of Algorithm 1.

## IV. NUMERICAL RESULTS

We consider  $M = 10$  antennas at the AP and a rectangular array of  $N = 80$  scattering elements at IRS. The AP-IRS, AP-receiver and IRS-receiver distances are given by 2,  $\sqrt{5}$ ,  $\sqrt{5}$  in meters, respectively. Furthermore, the path loss is modeled by the log-distance propagation model with the path loss exponent  $\alpha = 2$ . The path loss at the reference distance (1 m) is 30 dB. The energy harvesting efficiency is set as 0.8 and power consumption of a single scattering element is 15  $\mu\text{W}$  [12]. The AP's maximum transmission power is limited to 10 mW. We first give an illustrative example to show the convergence of the approximation algorithm for solving problem (P3). Its feasible region  $\Omega$  is illustrated in Fig. 2(a). It is clear that  $\Omega$  is a normal set by verifying the property in Proposition 1. As the objective of problem (P3) is increasing in both  $\gamma_0$  and  $r_1$ , we can adopt monotonic optimization to solve problem (P3) optimally. The convergent results of SPA algorithm for problem (P3) is shown in Fig. 2(b). We can observe that the lower and upper bounds, denote as  $r_L^{(k)}$  and  $r_U^{(k)}$ , respectively, converge fast in a few iterations, which verifies the effectiveness of the SPA algorithm.

Figure 3 shows the performance comparison of the proposed

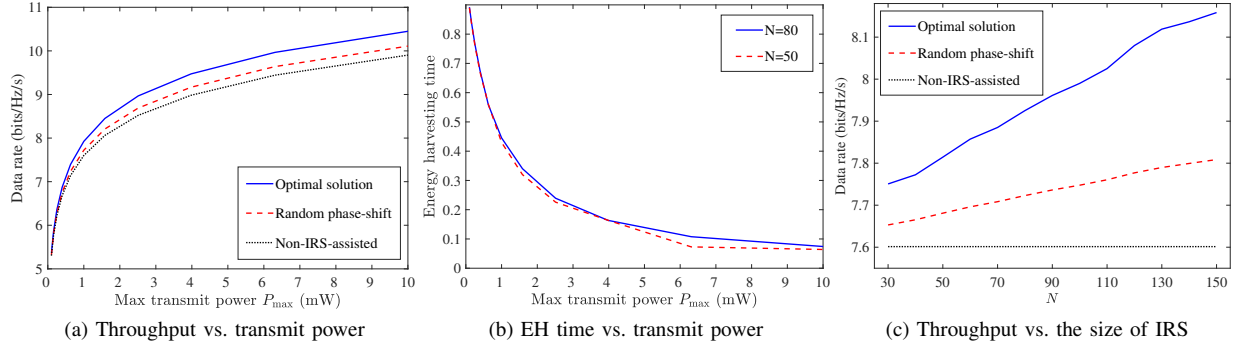


Figure 3: Optimal throughput and EH time vs. the AP's transmit power and the size of IRS.

system with some baseline approaches. We set different transmit powers at the AP and evaluate the throughput performance in both phases. For comparison, we also implement 1) a *random phase-shift* scheme that sets random passive beamforming for the IRS, 2) and a baseline scheme without using IRS. It is clear that our proposed system outperforms the random phase-shift scheme and the baseline scheme. The achievable throughput in three schemes are very close to each other when the AP's transmit power is relatively low. The performance gain of the proposed system becomes more significant with the increase of the AP's transmit power. In this case, the IRS can quickly harvest sufficient energy for its operation in the reflecting phase. Hence, the AP will experience more IRS-assisted information transmission with higher data rate. As shown in Figure 3(b), the IRS needs more time for energy harvesting when the AP's transmit power is small. In particular, the energy harvesting time takes up 90% of the unit time slot for  $p_{\max} = 0.1$  mW. Hence, the AP's information transmission is barely assisted by the IRS. For  $p_{\max} = 10$  mW, we can observe that the AP's information transmission can be IRS-assisted in most of the unit time slot, which leads to a more significant performance gain.

Figure 3(c) shows the performance gain with a different size of the IRS. It is clear that the overall throughput of the IRS-assisted system increases with the number of reflecting elements, for either the random phase-shift scheme or the optimal scheme. The performance gain in the optimal scheme raises from 2.0% to 7.3% compared to the baseline when the number of reflecting elements increases from 30 to 150. With more reflecting elements, the IRS has a higher flexibility to leverage the multi-path diversity and thus enhance the information transmission from the AP to the receiver.

## V. CONCLUSIONS

In this paper, we have investigated the throughput maximization problem of an IRS-assisted MISO system with a practical power budget constraint for the IRS. We propose a time-switching alike protocol for the IRS to harvest energy in the first phase and then assist information transmission in the second phase. The throughput maximization is formulated into a joint optimization of the AP's transmit beamforming in two phases, the IRS's time scheduling, and passive beamforming

strategies. Based on the problem structure, we decompose the original problem into two sub-problems that can be solved individually in two phases, respectively. The simulation results verify the superiority of the proposed system compared to the random phase-shift scheme and the baseline without IRS.

## REFERENCES

- [1] C. Liaskos, A. Tsioliaridou, A. Pitsillides, S. Ioannidis, and I. Akyildiz, "Using any surface to realize a new paradigm for wireless communications," *Commun. ACM*, vol. 61, no. 11, pp. 30–33, Oct. 2018.
- [2] S. Gong, X. Lu, D. T. Hoang, D. Niyato, L. Shu, D. I. Kim, and Y. Liang, "Towards smart wireless communications via intelligent reflecting surfaces: A contemporary survey," *IEEE Commun. Surv. Tut.*, pp. 1–1, Jun. 2020.
- [3] Q. Wu and R. Zhang, "Weighted sum power maximization for intelligent reflecting surface aided SWIPT," *IEEE Wireless Commun. Lett.*, pp. 1–1, Dec. 2019.
- [4] G. Yang, X. Xu, and Y. C. Liang, "Intelligent reflecting surface assisted non-orthogonal multiple access," in *proc. IEEE WCNC*, May 2020.
- [5] C. Huang, A. Zappone, G. C. Alexandropoulos, M. Debbah, and C. Yuen, "Reconfigurable intelligent surfaces for energy efficiency in wireless communication," *IEEE Trans. Wireless Commun.*, vol. 18, no. 8, pp. 4157–4170, 2019.
- [6] Q. Wu and R. Zhang, "Intelligent reflecting surface enhanced wireless network: Joint active and passive beamforming design," in *proc. IEEE Globecom*, Abu Dhabi, United Arab Emirates, Dec. 2018.
- [7] H. Shen, W. Xu, S. Gong, Z. He, and C. Zhao, "Secrecy rate maximization for intelligent reflecting surface assisted multi-antenna communications," *IEEE Commun. Lett.*, vol. 23, pp. 1488–1492, 2019.
- [8] L. Dong and H. Wang, "Secure MIMO transmission via intelligent reflecting surface," *IEEE Wireless Commun. Lett.*, pp. 1–1, Jan. 2020.
- [9] S. Gong, Y. Zou, D. T. Hoang, J. Xu, W. Cheng, and D. Niyato, "Capitalizing backscatter-aided hybrid relay communications with wireless energy harvesting," *IEEE IoT J.*, pp. 1–1, May 2020.
- [10] X. Zhou, R. Zhang, and C. K. Ho, "Wireless information and power transfer: Architecture design and rate-energy tradeoff," *IEEE Trans. Commun.*, vol. 61, no. 11, pp. 4754–4767, Oct. 2013.
- [11] R. Méndez-Rial, C. Rusu, N. González-Prelcic, A. Alkhateeb, and R. W. Heath, "Hybrid MIMO architectures for millimeter wave communications: Phase shifters or switches?" *IEEE Access*, vol. 4, pp. 247–267, 2016.
- [12] G. D. Vita and G. Iannaccone, "Design criteria for the RF section of UHF and microwave passive RFID transponders," *IEEE Trans. on Microw. Theory Techn.*, vol. 53, no. 9, pp. 2978–2990, Sept. 2005.
- [13] M. Grant and S. Boyd, "CVX: Matlab software for disciplined convex programming, version 2.1," <http://cvxr.com/cvx>, 2018.
- [14] H. Tuy, "Monotonic optimization: Problems and solution approaches," *SIAM J. Optim.*, vol. 11, no. 2, pp. 464–494, 2000.
- [15] J. Xu, Y. Zou, S. Gong, L. Gao, D. Niyato, and W. Cheng, "Robust transmissions in wireless-powered multi-relay networks with chance interference constraints," *IEEE Trans. Commun.*, vol. 67, no. 2, pp. 973–987, Feb. 2019.